Proceedings World Geothermal Congress 2015
Melbourne, Australia, 19-25 April 2015

Fluid Inclusion Gas Compositions of an Evolving Vapor-Dominated Geothermal System at Karaha - Telaga Bodas, Indonesia

Lorie M. Dilley and Joseph Moore

Hattenburg Dilley & Linnell, LLC, 3335 Arctic Blvd., Ste. 100, Anchorage, Alaska, USA 99517

Energy & Geoscience Institute, 423 Wakara Way, #300, Salt Lake City, Utah, USA 84108

ldilley@hdlalaska.com, jmoore@egi.utah.edu

Keywords: fluid inclusion gas chemistry, boiling, vapor zone, Karaha-Telaga Bodas

ABSTRACT

Variations in the compositions of gases trapped in fluid inclusions represent a unique source of information on the origins of the geothermal fluids and on the processes that have affected them. In this paper, we present data on fluid inclusion gases from the Karaha-Telaga Bodas geothermal system in west central Java. Wells up to 3 km in depth have encountered temperatures as high as 353°C and the underlying granodiorite that provides heat to the geothermal system. The gas compositions of fluid inclusions trapped in two wells, T-2 located near a vapor-chimney that allows magmatic gases to reach the surface and K-33, located in the central part of the system away from the chimney were studied. Vein filling minerals were analyzed for H_2, He, CH_4, H_2O, N_2, O_2, H_2S, Ar, CO_2, SO_2 and hydrocarbons (C_2-C_7). Fluid inclusions in bulk core samples that included the surrounding wall rock were analyzed for 180 masses including those listed above. Gas concentrations commonly range from >1.5 to 10 mole percent, although some of the inclusions contain gas contents exceeding 20 mole percent. Concentrations greater than 1.5 mole percent provide evidence of boiling, whereas contents greater than 10 mole percent are interpreted to indicate the presence of a gas cap. N_2/Ar ratios suggest fluid inclusions from T-2 contain significant contributions of magmatic gases whereas the gas compositions of fluid inclusions from K-33 suggest a meteoric origin. High gas concentrations in the fluid inclusions from both wells document the presence of a vapor phase and suggest the present-day steam zone was more extensive in the past. In T-2, gas-poor inclusions in the wall rocks underlie the steam zone and are interpreted as representing the early boiled fluid. Low gas fluid inclusions overlie the steam zone in both wells. These inclusions are interpreted to represent descending gas-poor condensate and meteoric waters that deposited calcite and anhydrite.

1. INTRODUCTION

Karaha-Telaga Bodas is a partially vapor-dominated geothermal system located on the flank of Galunggung Volcano, an active volcano that has erupted five times since 1822 (Figure 1). In the mid 1990s, Karaha Bodas Co. LLC drilled more than two dozen wells into the system, some to depths of 3 km. The wells encountered andesitic lava flows and volcaniclastic rocks that are underlain by a weakly altered granodiorite and temperatures as high as 353°C. The geometry of the geothermal system was described by Moore and others (2008) and is shown in Figure 2.

Four distinct hydrothermal mineral assemblages that document the evolution of the geothermal system and the transition from liquid- to vapor-dominated conditions were recognized (Moore and others, 2008). The earliest assemblage represents the initial liquid-dominated geothermal system generated during emplacement of the granodiorite between 5910 $\pm$ 76 and 4200 $\pm$ 150 y BP. Argillic, phyllic and propylitic alteration assemblages were formed by this system. Gravity temperature and mineralogic data suggest the granodiorite underlies the thermal area between Telaga Bodas and Kawh Kararah and provides the heat driving the system (Tripp et al., 2002; Moore and others, 2008). The intrusion is shallowest beneath the southern end of the field where Telaga Bodas, an acid lake overlies a nearly vertical low resistivity structure (<10 ohm-m) defined by magnetotelluric measurements. This structure is interpreted to represent a vapor-dominated chimney that provides a pathway to the surface for magmatic gases, including SO_2 and HCl. At 4200 $\pm$ 150 y BP, flank collapse and the formation of the volcano's crater, Kawah Galunggung (Katili and Sudradjat 1984), resulted in catastrophic decompression and boiling of the hydrothermal fluids. This event initiated development of the modern vapor-dominated regime. Chalcedony and then quartz were deposited as the early low salinity liquids boiled (assemblage 2). As pressures declined, CO_2-and SO_4-rich steam-heated water drained downward, depositing anhydrite and calcite (assemblage 3) in the fractures, limiting further recharge. Stage 4 is represented by the boiling off of the liquids in the southern part of the field, leading to the formation of Ti-rich scales on mineral and rock surface.

Fluid inclusions in quartz, anhydrite, calcite, wairakite, epidote and pyrite from four wells, T-2, T-8, K-21 and K-33 were analyzed to determine their temperatures of formations, salinities and gas contents. In this paper we compare and contrast fluid inclusion gas chemistry data from two of the wells, T-2 and K-33. These wells were selected for detailed analysis because of the extent of petrographic, microthermometric and gas data available from each. Gas analyses were conducted on both individual vein filling minerals and core samples that include vein minerals and the surrounding wall rock. Wells T-2 and T-8 are close to each other and represent similar geothermal environments. Similarly, K-21 and K-33 also represent environments similar to each other. Well T-2 was drilled to a depth of 1341 m on the northern side of Telaga Bodas (Figure 2) in 1997. The well did not penetrate the magmatic vapor chimney but did encounter a vapor-dominated conditions below 730 masl elevation. The well reached a temperature of 321°C. Well K-33 is located in the central part of the field where the steam zone is thin. It encountered a maximum temperature of 256°C. In contrast to T-2, K-33 encountered several organic-rich lake bed deposits near the base of the well.

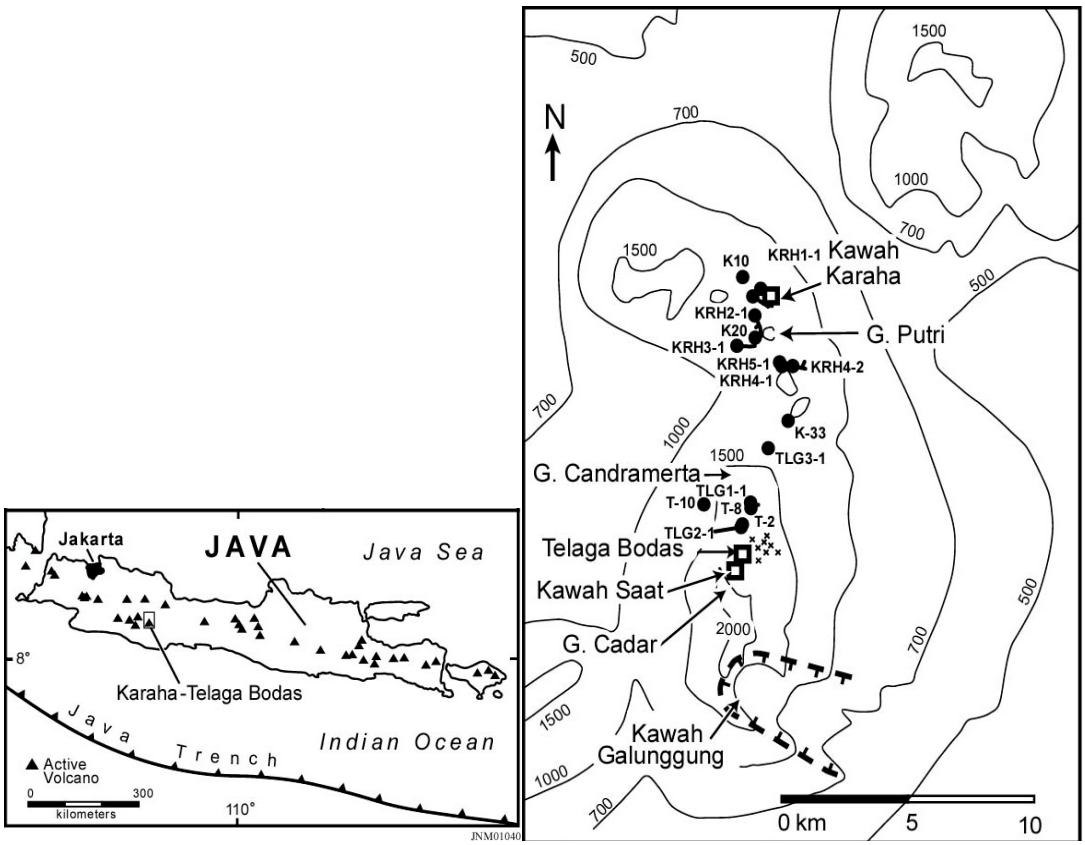

Figure 1. Location of Karaha-Telaga Bodas on the island of Java, and location of geothermal wells in relation to the volcanoes in the arc.

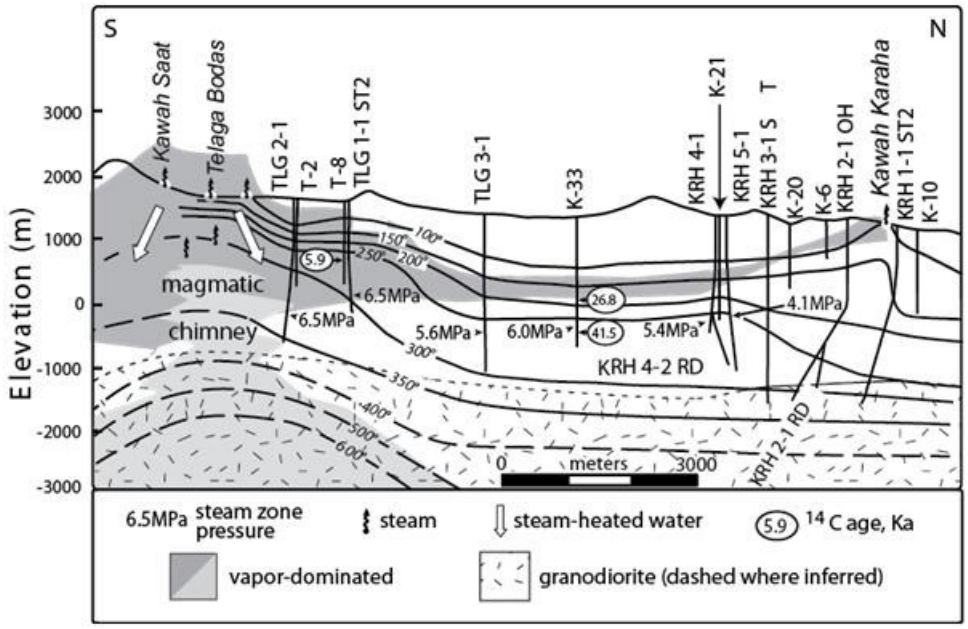

Figure 2:. Conceptual model of the geothermal system along the ridge axis showing temperature, distributions as a function of elevation in m above sea level, the geometry of the steam and liquid zones based. on flow tests and downhole measured pressures. Temperatures are shown as solid lines where measured and dashed where inferred. Regions in shades of gray are vapor-dominated. The magmatic vapor-dominated chimney is shown in light gray; surrounding portions of the vapor-dominated zone are dark gray. From Moore et al. (2008)

The vein minerals were handpicked and analyzed at New Mexico Tech (samples labeled NMT). The gases were released under vacuum and analyzed by quadrupole mass spectrometer H_2, He, CH_4, N_2, O_2, H_2S, Ar, CO_2, SO_2 and hydrocarbons (C_2-C_7). Multiple crushes were performed on each sample. The analytical techniques are described by Norman and Sawkins (1987), The data are reported in mole percent. In contrast, the core samples were crushed once before being analyzed by quadrupole mass spectrometry. These analyses provide information on the fluid-dominated environment present in the veins.

The bulk analyses of the core samples were conducted by Fluid Inclusion Technology (samples labeled FIT). Each sample was crushed once and analyzed by quadrupole mass spectrometry for 180 masses including those measured at NMT. These samples provide information on the rock-dominated environment that characterizes the bulk of the geothermal system. The FIT analysis yields counts for each chemical species. The more abundant the chemical species the higher the count; however the count cannot be converted into a mole percent or other standard measurement unit. In this study, we use the relative concentrations of individual gas species to display the data on ternary plots and total gas concentrations that are above or below the average value in the well to display gas contents. We show that the two data sets yield similar trends and interpretations consistent with the geologic model of the geothermal system. We then use the fluid inclusion gas chemistry to determine fluid types within each well.

2. FLUID INCLUSION STUDIES

Microthermometric measurements and gas analyses were conducted on quartz, calcite, anhydrite and fluorite. In addition, gas analyses were performed on pyrite. Approximately 1800 quartz-hosted inclusions from more than 30 depth intervals in T-2, T-8, K-21 and K33. With the exception of quartz from 529 masl elevation in T-8, only two phase liquid and vapor-rich inclusions were observed. Fluid inclusions from this sample contain liquid, vapor and solid phases.

Liquid- and vapor-rich inclusions were observed in nearly every quartz crystal studied and growth zones containing large primary vapor-rich inclusions are common in many of the samples (Figure 3). Because liquid must have been present as the quartz crystals grew, these primary fluid inclusions are taken as evidence of boiling at the sample site. Liquid-rich fluid inclusions trapped in quartz record temperatures ranging from 123^{o} to 348^{o}C. The distribution of homogenization temperatures of individual fluid inclusion assemblages with respect to elevation and the measured downhole temperatures are plotted in Figure 4. Because it can be inferred that the fluids were boiling at the time of quartz deposition, the homogenization temperatures of primary fluid inclusions, and possibly many of the secondary inclusions, represent the true trapping temperatures (Roedder and Bodnar, 1980).

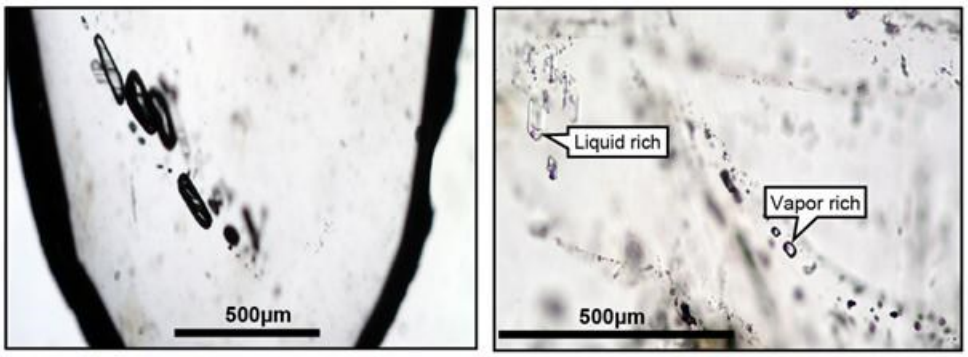

Figure 3: Left: Vapor rich inclusions in quartz crystals. Right: Liquid- and vapor-rich inclusions trapped on different healed fractures.

Temperature-salinity relationships are shown in Figure 4. The highest salinity fluids, ranging up to 26 weight percent NaCl-$CaCl_2$ equivalent, were trapped in quartz from T-8, although high salinities are also found in a sample from an intermediate depth in T-2. In contrast, salinities in K-21 and K-33 do not exceed ~2 weight percent NaCl equivalent. The high salinities in T-2 and T-8 are interpreted to record the progressive boiling off of the early liquid-dominated geothermal system. As discussed below, salinities near 0 weight percent NaCl equivalent are interpreted to represent condensate.

Temperature-depth and temperature salinity relationships of fluid inclusion assemblages in anhydrite, calcite and fluorite from T-2, T-8, K-21 and K-33 are shown in Figure 5. Two phase liquid-rich inclusions dominate, although both vapor rich and rarely three phase liquid-rich inclusions containing halite are present. Homogenization temperatures range from 108^{o} to 308^{o}C, and with few exceptions closely mimic the measured temperatures, suggesting recent trapping..

Fluid inclusions from T-2 and T-8 display a progressive change in their composition and temperature with depth (Moore et al, 2004a). As shown in Figure 5, salinities initially decrease as temperatures increase to 205^{o}C. The salinities then remain nearly constant as the homogenization temperatures increase further to 235^{o}C. At this point, the trend reverses and the salinities increase with increasing temperature. The progressive decrease in salinity is attributed to the incorporation of SO_4 into the newly formed hydrothermal minerals. This mechanism does not, however, provide an explanation for the subsequent increase in salinity with increasing temperature.

The highest salinities are found in anhydrite deposited near the top of the vapor-dominated zone (sample from 586 m elevation in T-8). Anhydrite from this depth is coated with Ti-rich precipitate. Both vapor-rich and three phase halite-bearing liquid-rich inclusions were trapped. The three-phase inclusions homogenize to the liquid phase by disappearance of the vapor bubble at temperatures ranging from 283^{o} to 308^{o}C (average 297^{o}C; n = 18). Halite dissolution temperatures yield a salinity of 31 weight percent NaCl equivalent.

In contrast to inclusions from T-2 and T-8, the salinities of inclusions from K-33 and K-21 show little variation with depth or temperature. All but one inclusion yielded a salinity between 0.0 and 0.9 weight percent NaCl equivalent (n = 176). Salinities near 0.0 are typical of fluid inclusions that trap steam condensate (Moore et al, 2000a) and dilute meteoric water. The trapping of condensate is supported by occurrences of corroded quartz crystals. In actively convecting geothermal systems, fluids rapidly equilibrate with quartz within days to weeks (Rimstidt and Barnes, 1980) Thus, dissolution of quartz implies interactions with fluids whose circulation paths are relatively short. The relatively high homogenization temperatures of these inclusion fluids

suggest they are more likely to represent low salinity steam condensate generated near the site of quartz dissolution than cool, rapidly descending shallow groundwater.

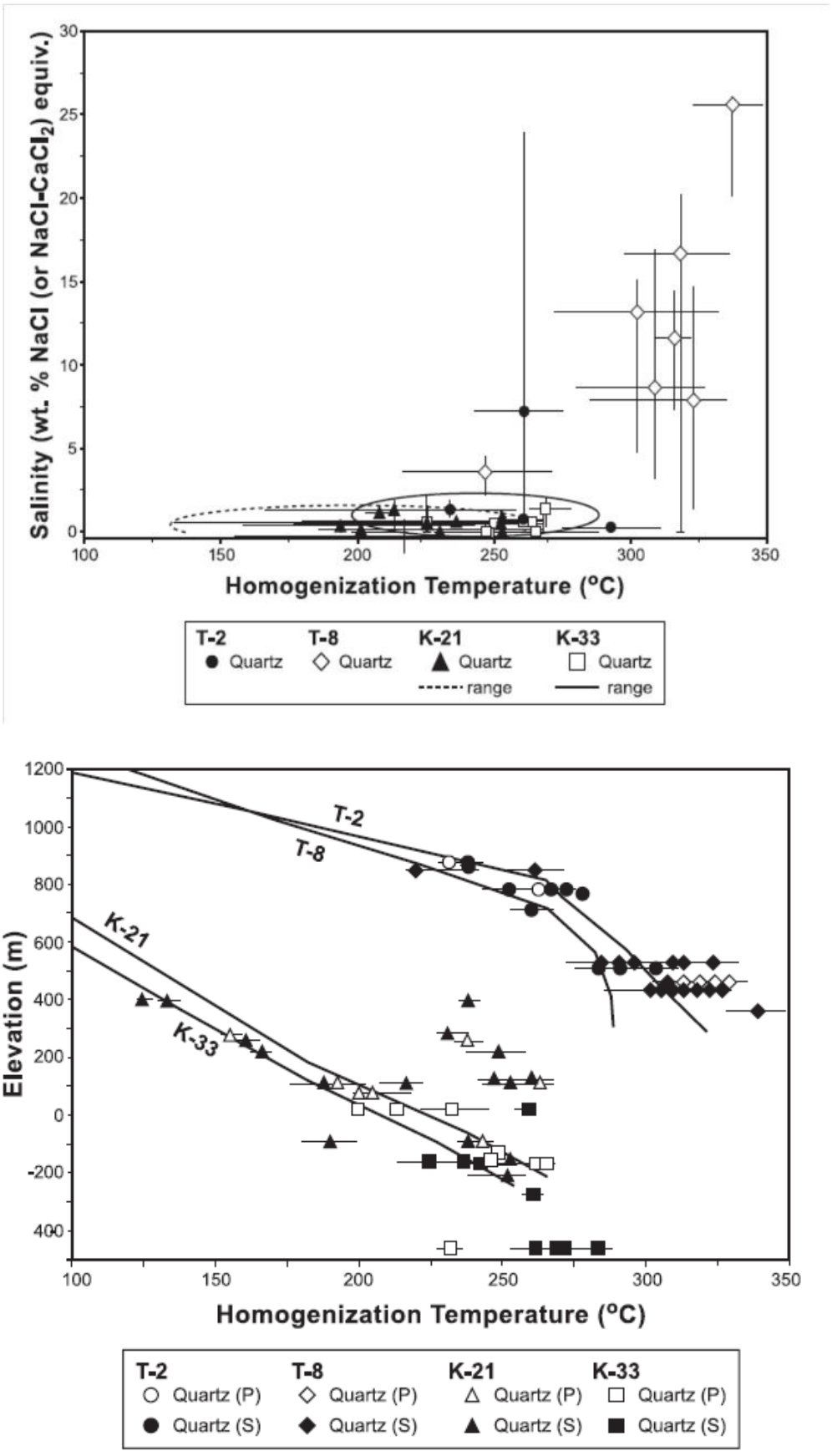

Figure 4. Temperature salinity and temperature-depth relationships of fluid inclusion assemblages in quartz from T-2, T-8, K-21 and K-33.

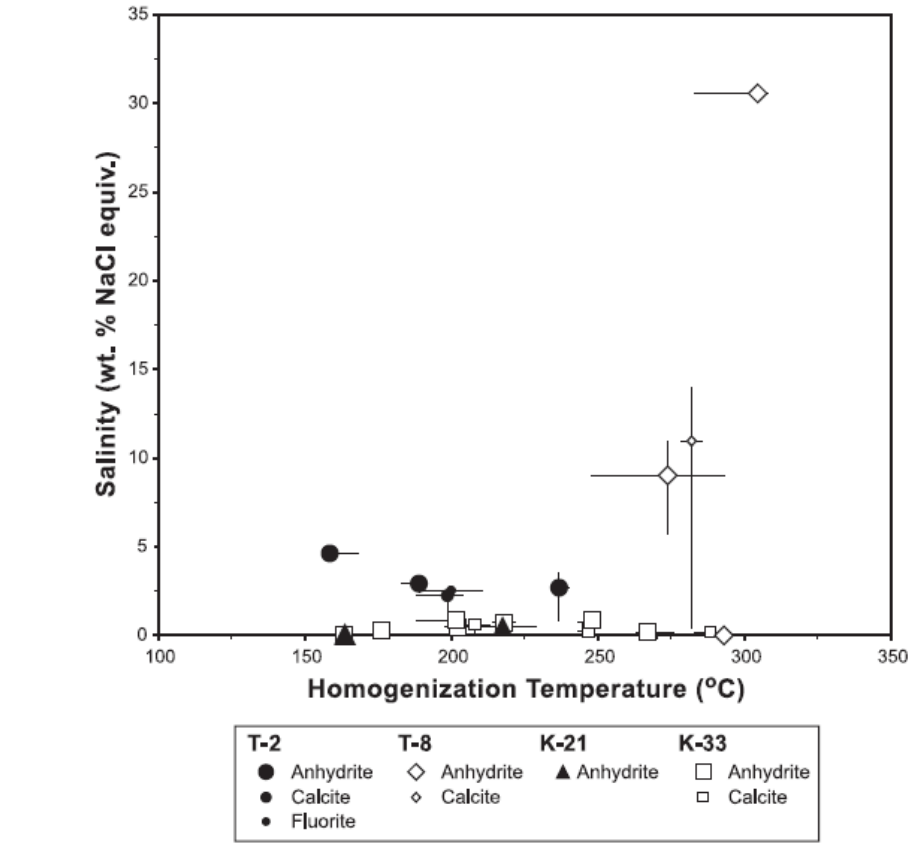

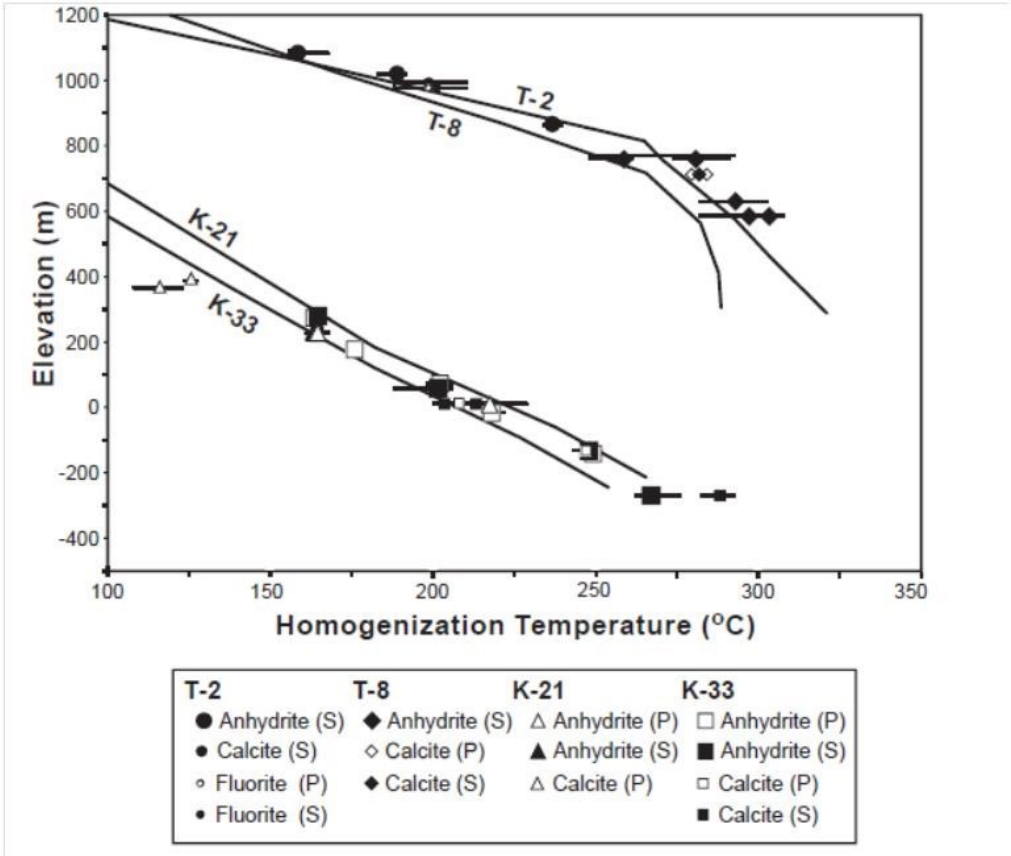

Figure 5. Temperature salinity and temperature-depth relationships for fluid inclusion assemblages in anhydrite, calcite and fluorite from T-2, T-8, K-21 and K-33.

3. FLUID INCLUSION GAS ANALYSES

Carbon dioxide (CO_2), hydrogen sulfide (H_2S), hydrogen (H_2), nitrogen (N_2), methane (CH_4), and inert gases are the major gaseous species in geothermal fluids (Ellis and Mahon 1977; Henley and others. 1984). Previous work on interpreting fluid sources and fluid processes from geothermal gas chemistry has shown the following: (1) meteoric-air saturated water (shallow groundwater) has low concentrations of gaseous species and N_2/Ar ratios of between 38 to 54; (2) reservoir fluids that are the deeply circulating alkaline chloride waters typically have N_2/Ar ratios greater than air, CO_2/CH_4 ratio greater than four (if the reservoir rocks are low in organic matter, and H_2S contents close to equilibrium with pyrite and magnetite; (3) boiling creates inclusions enriched in gas; (4) condensation results in concentrations of more soluble gaseous species including H_2S, CO_2, and aromatic organic species; (5) low permeability zones are characterized by low concentrations of fluid inclusions and below average values for all species of interest; and (5) fluid inclusion gas analyses can be interpreted using standard geochemical techniques (Giggenbach, 1986; Henley, 1985: Henley et al, 1984; Norman and Musgrave 1994; Dilley, 2009).

3.1 N_2-Ar-He relationships of FIT analyses

The N_2-Ar-He diagram compares the relative gas contents derived from magmatic, crustal, and meteoric sources (Figure 6). Although the value of the N_2/Ar ratios in a bulk sample cannot be determined directly, the relative values of the N_2/Ar ratios can provide an indication of the fluid source. Figure 7 show the relative N_2-Ar-He concentrations for FIT analysis for T-2 and K-33 respectively. The analyses from T-2 are significantly enriched in N_2 relative to those from K-33, suggesting the fluids have different origins. The mixing trend is more towards the N_2 apex in T2 than in K33.

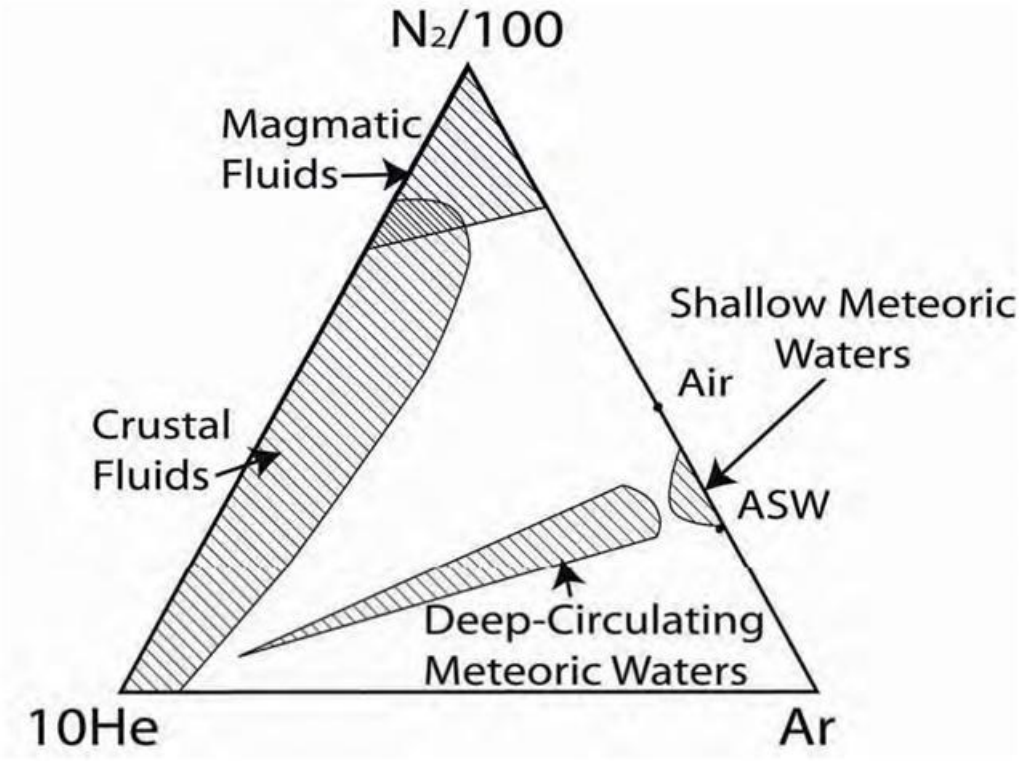

Figure 6. N2-Ar-He compositional fields for magmatic, crustal, deeply circulated meteoric, and shallow meteoric fluid sources (modified from Norman and Musgrave 1994).

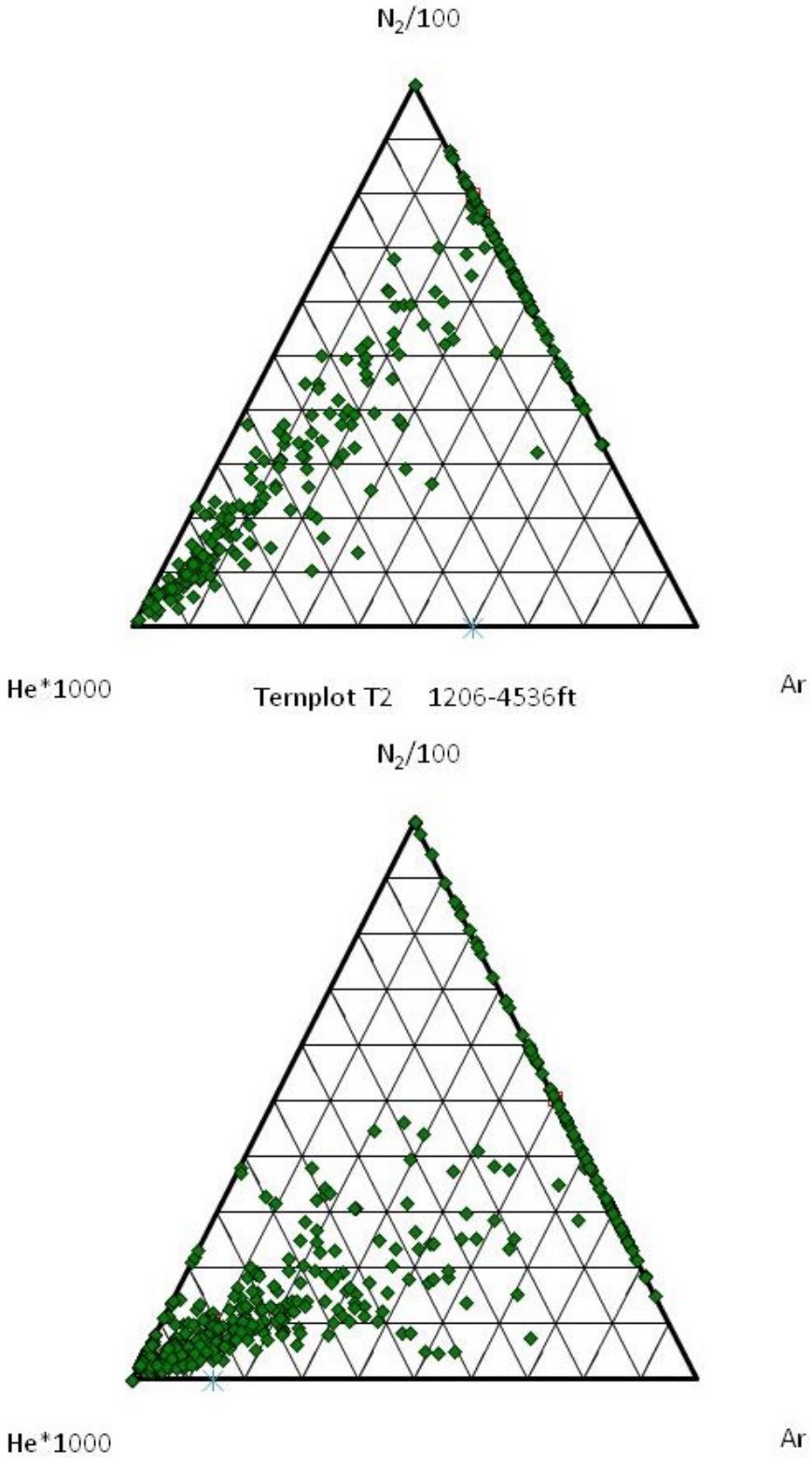

Figure 7. N_2-He-Ar ternary diagram for T-2 and K-33. Note the high N_2/Ar ratios in T-2 as oppose to K-33 and trend extending from the He apex.

3.2 Fluid Inclusion Logs

Logs based on selected chemical species were generated from the fluid inclusion gas chemistry from the bulk samples for each well. Fluid types were interpreted based on the chemical signatures for each sample (Dilley, 2009). Figures 8 and 9 shows the fluid types by color: meteoric water in blue; background fluids in gray; two-phase fluids in yellow; and fluids with magmatic components in purple. The background fluid type is used to represent the fluid inclusion gas chemistry prior to the influx of geothermal or meteoric fluids. Zones of fluid types can then be interpreted based on the results.

The fluid log for K-33 (Figure 8) shows higher concentrations of helium, organic compounds, and sulfur species than the fluid log for T-2 (Figure 9). H_2O (shown in light blue) is also higher in concentration than in T-2. Total gas concentrations are higher in K-33 than in T-2 particularly near the bottom of K-33.

3.3 Total Gas

Total gas versus elevation was plotted for the two wells using both NMT and FIT datasets as shown in Figure 10. As noted, the FIT analysis is not quantitative To compare the analyses, the FIT total gas concentration was calculated using the same species as NMT for each sample. The total gas was divided by 1,000,000 in order to plot on the same graph as the NMT data. The FIT data was color coded for those total gas concentrations above the average concentration (blue) and those below the average concentration (brown). The NMT data is plotted in mole percent. In each figure, the top of the present-day steam zone is indicated by the horizontal line; in K-33, the bottom of the steam zone is also shown. The vertical line at 1.5 mole percent gas provides a conservative estimate of the gas content of a single phase liquid, only in reference to NMT data. Concentrations greater than 1.5 mole percent indicate the presence of a vapor phase trapped in the fluid inclusions.

The FIT data from T-2 indicates above average total gas concentrations occur above the top of the present-day steam zone and coincident with the top of the high gas-bearing fluid inclusions defined by the NMT analyses. This occurs at approximately 900 masl A similar depth is indicated by the presence of two-phase fluids in the interpreted log shown in Figure 9.

In K-33, the FIT and NMT data show above average concentrations of gases from approximately 200 masl to the total depth of the well (see also distribution of two-phase zone in Figure 9). Both data sets indicate gas-rich fluid inclusions were trapped above and below the present-day steam zone.

4. INTERPRETATION

Although the overall mineral relationships suggest the rocks in T-2 and K-33 have undergone similar evolutions the fluid inclusion gases suggest there were significant differences in the geothermal environments at T-2 compared to K-33. Fluid inclusions in T-2 are characterized by higher N_2/Ar concentrations (commonly above 200) and CO_2/CH_4 ratios above 4. These ratios suggest the presence of a significant magmatic component in the inclusion fluids. Two different environments are suggested by the vein minerals whereas the bulk FIT data suggest a third environment developed in the wall rocks at depth. Both data sets indicate the trapping of a gas-poor fluid above 900 masl. Based on the occurrences of anhydrite and calcite and the fluid inclusion salinities and temperatures, the shallow fluid is interpreted to be steam condensate. The veins contain gas-rich inclusions to the total depth of the well, suggesting boiling and gas movement was occurring in these channels. In contrast, FIT analyses of inclusions from elevations below 600 masl indcate lower total gas concentrations than the two-phase fluid above, suggesting these inclusions trapped a degassed and boiled reservoir.

In contrast to T-2, the fluids in K-33 trapped a lower N_2/Ar fluid (refer to Figure 7), K-33 inclusions are also generally less saline than inclusions in T-2. As in T-2, fluids above 200 masl have low gas contents. Veins in these rocks have deposited anhydrite and calcite, suggesting the fluids are downward percolating condensate. However, the relatively low N_2/Ar ratios and the fluid inclusion chemistry suggests the source of the condensate was meteoric water. At greater depths, the chemistry and gas contents indicate the presence of two-phase fluids. The organics (shown in green in Figure 8) are most likely the result of pyrolysis of organic matter in the lake bed deposits.

The fluids from both T-2 and K-33 contain significant concentrations of He. Neither the NMT or FIT analyses can distinguish ^{3}He from ^{4}He thus it is not possible to determine if there is a magmatic contribution to the He contents of the inclusions. Chemical analyses of the gas actively being discharged indicate there is a significant flux of magmatic He (7.1-7.7 Ra) (Moore and others, 2008). Thus it is likely there is a significant contribution of magmatic He to the fluids trapped in T-2 and K-33.

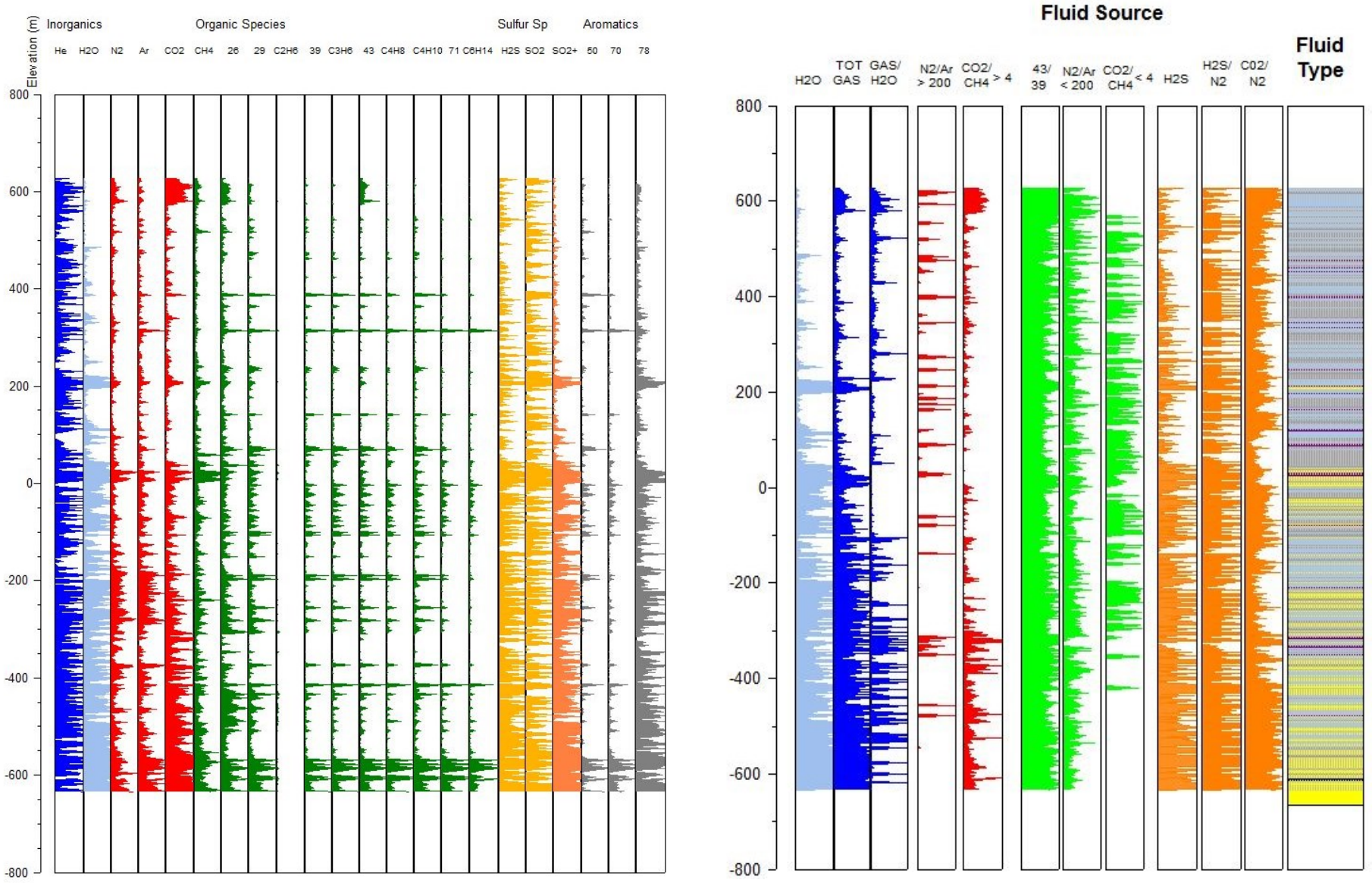

Figure 8. Fluid inclusion log for K33.

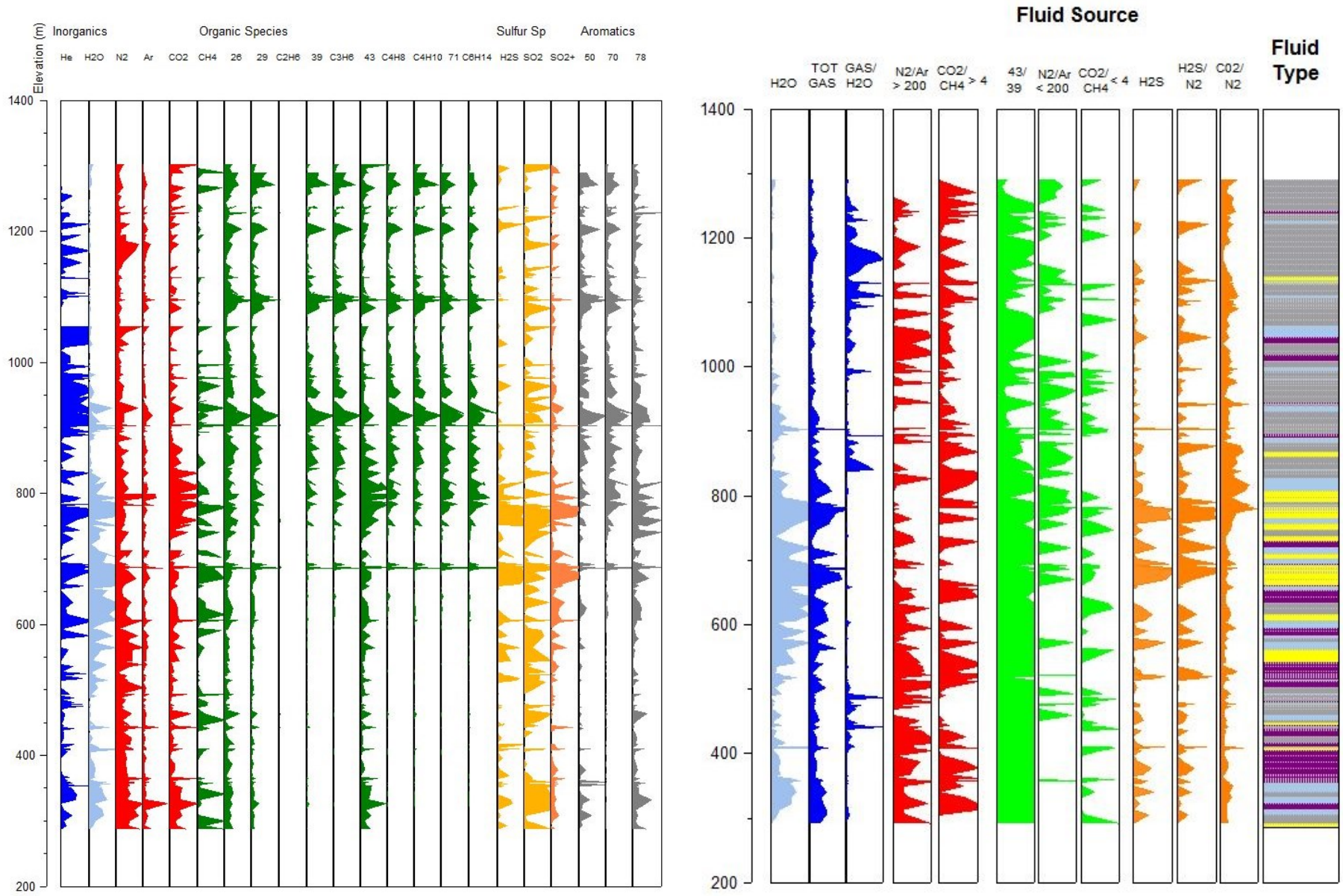

Figure 9. Fluid log for T2.

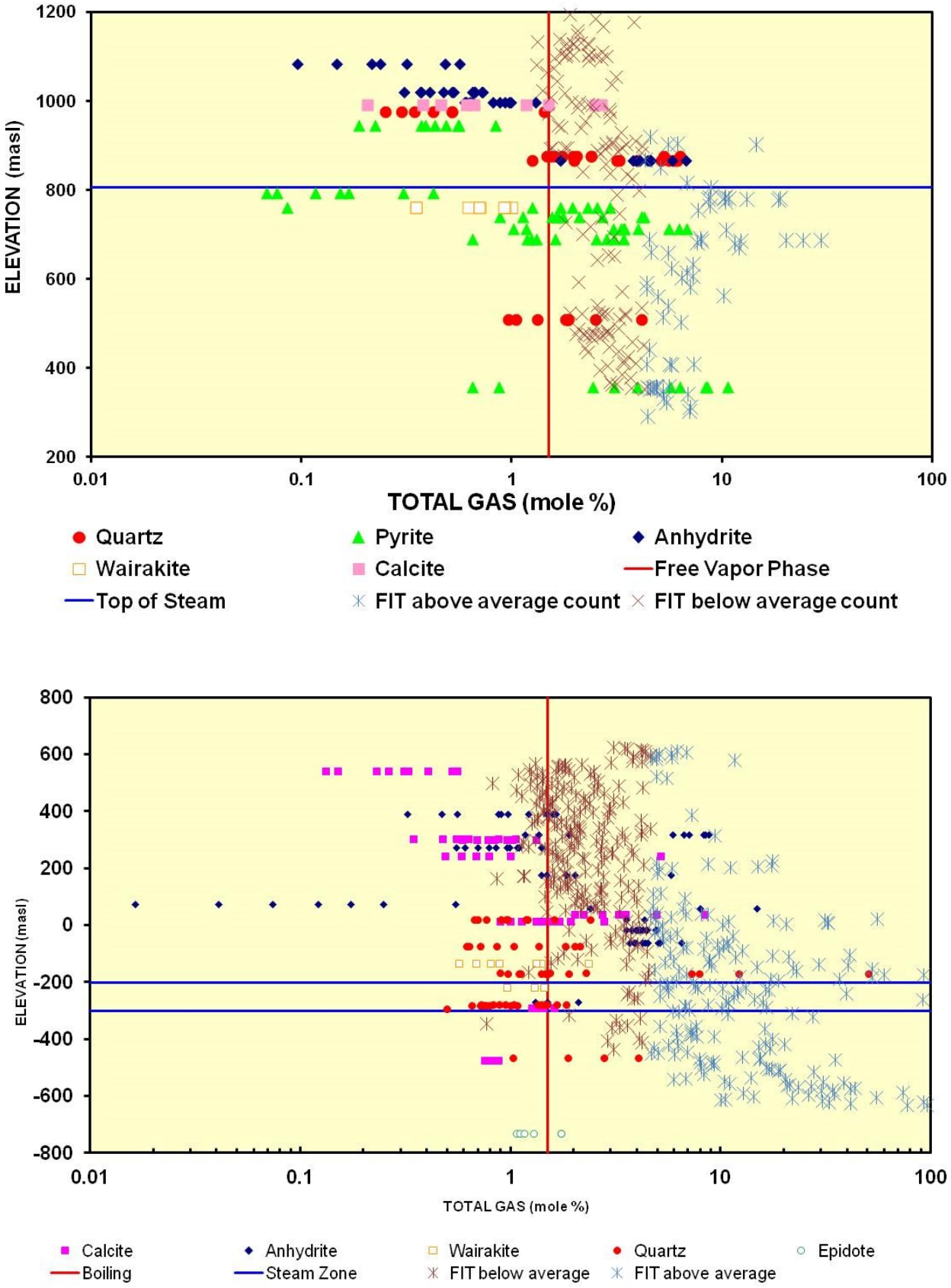

Figure 10. Total gas versus Elevation for T2 (top graph) and K33 (bottom graph). The FIT data was divided into below average concentration and above average concentration in both wells.

5. CONCLUSIONS

This study documents the utility of bulk fluid inclusions analyses in interpreting reservoir processes. The following conclusions can be drawn from this study.

1. Fluid inclusion gas analysis conducted on bulk samples at Karaha-Telaga Bodas provide an important record of geothermal processes that have occurred during the evolution of the system.
2. Although the bulk analyses are qualitative, when combined with mineralogic and fluid inclusion microthermometric data, they can provide interpretations consist with quantitative data obtained on individual crystals.
3. Variations in relative N_2-Ar-He and total gas contents provide information on fluid sources, magmatic contributions and boiling. At Karaha-Telaga Bodas, the data indicate that gases trapped in T-2, close to a vapor-chimney are enriched in magmatic gases whereas fluids trapped in K-33, located near the center of the field, are dominantly meteoric in origin.
4. Bulk gas analyses of the wall rocks are interpreted to provide information on fluid compositions trapped in rock-dominated environments whereas analyses of vein minerals provide information on fluid-dominated environments. Fluid inclusions trapped in vein minerals from T-2 contain higher gas contents than the bulk wall rock from comparable depths. These low gas contents of the wall rock fluid inclusions are interpreted to represent boiled and degassed fluids whereas the compositions of the vein minerals show evidence of a separate gas phase.

ACKNOWLEDGEMENTS

The authors are grateful to the management and staff of the Karaha Bodas Co. LLC for generously providing the samples and data used in this investigation. Funding for LMD was provided by the Department of Energy under contract DE-EE0005519.001.

6. REFERENCES

Dilley, L.M. (2009). Fluid Inclusion Stratigraphy A New Method for Geothermal Reservoir Assessment, PhD Dissertation, New Mexico Institute of Mining and Technology.

Giggenbach, W. F. (1986). The use of Gas Chemistry in Delineating the Origin of Fluid Discharges over the Taupo Volcanic Zone: A Review. International Volcanological Congress, Hamilton, New Zealand Proceedings Seminar 5: 47-50.

Henley, R.W. (1985). The Geothermal Framework for Epithermal Deposits. In B.R. Berger and P.M. Bethke (eds), Geology and Geochemistry of Epithermal Systems: Reviews in Economic Geology, vol. 2, Society of Economic Geologists, pp. 1-24.

Henley, R.W., Truesdell A.H., and P.B. Barton, Jr. (1984). Fluid-Mineral Equilibria in Hydrothermal Systems, Reviews in Economic Geology, vol. 1, Society of Economic Geologist, 267 pp.

Katili, J.A,. and Sudradjat A. (1984). Galunggung: the 1982-1983 eruption. Bandung: Volcanological Survey of Indonesia

Moore, J.N, Allis, R.G., Nemčok, M., Powell, T.S., Bruton, C.J., Wannamaker, P.E., Raharjo, I.B. and Norman, D.I., (2008). The evolution of volcano-hosted geothermal systems based on deep wells from Karaha - Telaga Bodas, Indonesia: American Journal of Science, v. 308, p. 1-48.

Norman, D.I., and Musgrave, J. (1994) N2-Ar-He compositions in fluid inclusions: indicators of fluid source. Geochemica Cosmochimica Acta, v. 58, p. 1119-1131.

Norman, D.I., and Sawkins, F.J., (1987) Analysis of gases in fluid inlcusions by mass spectrometer. Chemical Geology, vol 61, p. 10-21.

Rimstidt, J. D., and Barnes, H. L., 1980, The kinetics of silica-water reactions: Geochimica et Cosmochimica Acta, v. 44, p. 1683-1699.

Roedder, E., and Bodnar, R. J., 1980, Geologic pressure determinations from fluid inclusion studies: Annual Reviews in Earth and Planetary Sciences, v. 8, p. 263–301.

Tripp, A., Moore J., Ussher G., McCulloch J. (2002). Gravity Modeling of the Karaha-Telaga Bodas Geothermal System, Indonesia, Proceedings: Twenty-second Workshop of Geothermal Reservoir Engineering, Stanford University, Stanford, California.